



TECHNICAL ARTICLE

# On Selected Properties of Inconel 625/Ti6Al4V Explosively Welded Clad

Joanna Wojewoda-Budka , Monika Bugajska, Jan Guspiel, Sylwia Terlicka, Agnieszka Bigos, Anna Wierzbicka-Miernik, and Zygmunt Szulc

Submitted: 26 November 2021 / Revised: 19 March 2022 / Accepted: 3 April 2022 / Published online: 3 May 2022

This study presents the microstructure and physicochemical properties of explosively welded Inconel 625 and Ti6Al4V platers, which were investigated by scanning electron microscopy, corrosion resistance, and dilatometric measurements. Firstly, the corrosion behavior of Ti6Al4V was tested in sodium sulfate and sodium chloride solutions using potentiodynamic polarization and electrochemical impedance spectroscopy techniques. The experimental results were compared with the data obtained from computer simulation. The investigated corrosion resistance of the explosively welded Inconel 625/Ti6Al4V system in different solutions showed that this system exhibited significantly higher corrosion resistance in NaCl solution than in sodium sulfate. In addition, the corrosion potential of the Ti6Al4V surface tested in sodium chloride is slightly higher compared to the value obtained for the second solution. Moreover, the pioneering dilatometric measurements have been carried out in the temperature range of 298–873 K to determine the linear coefficient values of thermal expansion ( $\alpha$ ) of investigated samples cut along and perpendicular to the direction of the explosion. They showed close values regardless of the cutting direction. Additionally,  $\alpha$  possessed the linear character in the whole investigated temperature range, excluding the phase transitions within the bonded plates.

**Keywords** corrosion, explosive welding, Inconel 625, potentiodynamic polarization technique, Ti6Al4V, thermal expansion

## 1. Introduction

Titanium and titanium alloys have unique properties compared to other engineering materials due to their high relative strength over a wide temperature range, additionally being non-magnetic, biocompatible, and high corrosion resistant (Ref 1). Regarding chemical and process apparatus, the most important property is corrosion resistance, which is the main criterion for the selection of a given material to work in a specific, chemically aggressive environment. Therefore, titanium and titanium alloys attract much attention and are increasingly used despite their high cost of production (Ref 2). These costs can be

compensated by the use of titanium explosive plating technology, which is a major contributor to the widespread use of titanium in engineering designs. This welding technology can not only reduce the cost of production but also provide other valuable properties.

The present work is dedicated to the structural, electrochemical, and physical studies of explosively welded platers of high-melting titanium (Ti6Al4V) and nickel (Inconel 625) alloys. The examined combination of Ti6Al4V (used for protection of nickel alloys against oxidation in elevated temperatures) with nickel Inconel 625 alloy (resistant to high temperature) can be applied in marine engineering where high corrosion resistance at different temperatures combined with good mechanical strength is required (Ref 3, 4), as well as in the aerospace industry in components where resistance to long-lasting high temperature plays an important role (Ref 5–7). In such combinations, explosive welding (EXW) technology can be an efficient way of joining such materials, especially due to the jetting phenomenon, that cleans the surfaces right before joining (Ref 8, 9). Moreover, these welding processes take place under extreme conditions of pressure and temperature, and hence the product characteristics and any properties of the newly formed materials must be carefully studied. One of the important issues from the point of view of modern engineering materials obtained by the EXW method is to study their corrosion resistance after strong impact generated during the welding and thermal expansion measured for the complete weld, as well as the materials forming it. However, the data of the corrosion resistance of the severely deformed titanium alloy together with the thermal expansion coefficient of the investigated explosively welded platers are still not known. The only existing literature for this explosively welded configuration of materials focuses only on the description of microstructure

This article is an invited submission to the *Journal of Materials Engineering and Performance* selected from presentations at the symposium “Wetting, High-Temperature Capillarity, Interface Design and Modeling,” belonging to the area “Processing” at the European Congress and Exhibition on Advanced Materials and Processes (EUROMAT 2021), held virtually from September 12–16, 2021, and has been expanded from the original presentation.

Joanna Wojewoda-Budka, Monika Bugajska, Jan Guspiel, Sylwia Terlicka, Agnieszka Bigos, and Anna Wierzbicka-Miernik, Institute of Metallurgy and Materials Science, Polish Academy of Sciences, 25 Reymonta St., 30-059 Krakow, Poland; and Zygmunt Szulc, High Energy Technologies Works “Explomet”, 100H Oświęcimska St., 45-641 Opole, Poland. Contact e-mail: j.wojewoda@imim.pl.

correlated with the mechanical properties (Ref 6) of newly formed weld, the study of which is important as a first stage.

Hence, in the present work, for the first time, the corrosion studies of the Inconel 625/Ti6Al4V system obtained by explosive welding have been carried out, which have not been presented in the literature before. In this paper, corrosion studies were carried out on the outer surface of the plater composed of Ti6Al4V alloy, because this surface will be exposed to long-term high temperatures or aggressive corrosive environment in practical application.

Moreover, this study also presents, for the first time in the literature, measurements of the linear thermal expansion coefficient of explosively welded Ti6Al4V and Inconel 625 plater, in the range from room temperature to 873 K. These measurements allow future prediction of the behavior of such a materials' combination under operating conditions.

## 2. Materials and Methods

The Ti6Al4V sheet with a thickness of 0.84 mm (flyer plate) was explosively welded with the Inconel 625 sheet with a thickness of 1.55 mm (base plate). The chemical composition of the welded materials can be found in Table 1. In the present configuration, the flyer plate (Ti6Al4V) was accelerated by the impact of a high-velocity explosion toward the base plate (Inconel 625), which was on the ground. As a result of the impact, a permanent bond was formed at the plate boundary, the morphology of which has been described in this paper and also in (Ref 6). A schematic representation of the joining process is shown in Fig. 1. The parameters used to obtain the weld presented in this paper remain a trade secret of "Explomet" company, that provides the study material and therefore are not given.

Microstructure and chemical composition changes across the joined zone were analyzed using a scanning electron microscopy (SEM, ESEM XL30, FEI) working at an accelerating voltage of 20 kV and equipped with an energy-dispersive x-ray spectrometer (EDS, EDAX).

Corrosion measurements were performed with an AUTOLAB PGSTAT302N potentiostat/galvanostat. Each experiment was controlled using the commercial NOVA 2.1.4 software. The electrochemical measurements were conducted at 298 K in a Pine thermostatic cell, using a standard three-electrode system. This system consisted of a working electrode, which was the investigated material, a saturated calomel electrode (SCE) (placed in a Luggin capillary) used as a reference electrode, and platinum auxiliary electrodes. The total area of the platinum electrodes was 4.5 cm<sup>2</sup>. 24 h before measurements, the surface of the samples was prepared by grinding on SiC-based papers (starting with 800, then 1000, 2000, and finally 7000 gradations) for 2 min. Just before starting the tests, the side surface of the sample was protected with a non-conductive layer, leaving only a working area, which was 0.27 cm<sup>2</sup>, for immersion. Two different solutions

were used during the measurements. The first one was a 0.5 M aqueous solution of Na<sub>2</sub>SO<sub>4</sub> with a pH of 6.0, and the second one was a 0.5 M aqueous solution of NaCl, whose pH value was corrected to 7.0. Then 500 ml of Na<sub>2</sub>SO<sub>4</sub> or NaCl solution (aerated for 20 minutes) was placed in the electrochemical cell. The open-circuit potential ( $E_{OCB}$ ) was measured as a function of time during the 1800 s. This time was sufficient to establish the constant value of  $E_{OCB}$ . The anodic and cathodic branches were recorded by polarizing the sample within  $\pm 120$  mV with respect to  $E_{OCB}$  with a scanning rate of 1 mV/s. The corrosion potential ( $E_{corr}$ ) and corrosion current ( $i_{corr}$ ) were determined from the voltammetric curves. The polarization resistance ( $R_p$ ) was calculated using the Stern-Geary Eq 1:

$$R_p = \frac{b_a \cdot b_c}{2.3 \cdot (b_a + b_c) \cdot i_{corr}} \quad (\text{Eq 1})$$

where  $b_a$  and  $b_c$  are the slopes of the anode and cathode sections of the polarization curve, respectively.

The electrochemical impedance spectroscopy (EIS) measurements were also performed at a potential with an amplitude of 10 mV and a frequency varying in the range of 30 kHz-0.1 Hz. The results of impedance tests were presented as a Nyquist plot. The impedance characteristics were determined by approximating the experimental data with physical and mathematical electrical equivalent circuit models using the commercial Nova 2.1.4 software.

The thermal expansion of explosively welded platers made of nickel and titanium alloys (that is, Inconel 625 and Ti6Al4V) was measured using an optical, horizontal dilatometer, Misura 3 FLEX-ODLT. All measurements were performed analogously to those presented in the works (Ref 10, 11). All specimens were examined over a temperature range from 298 to 873 K in the air atmosphere, using a heating rate of 10 K/min. During the thermal expansion tests, each 5 × 5 × 50 mm parallelepiped shaped sample was placed horizontally in the furnace of the dilatometer on a ceramic plate placed on two alumina rods. The dilatometer is equipped with two high-resolution monochromatic cameras (*iCube* from NET GmbH), which accurately record the changes of the sample edges as the measurement temperature increases. The temperature and expansion properties of this device are calibrated periodically using Standard Reference Material 738 - Stainless Steel (AISI 446, NIST). The temperature error in the thermal expansion measurements was estimated to be  $\pm 2$  K.

## 3. Results and Discussion

### 3.1 Microstructure Observation

The microstructure observations of the Inconel625/Ti6Al4V interface were the starting point of this study. Although the continuity throughout the observed length of samples was

**Table 1 The chemical composition of the Inconel 625 and Ti6Al4V (Ref 6)**

Element	Ni	Cr	Fe	Al	Ti	V	Mo	Nb	C	Mn	Si
Inconel 625 (% wt.)	Base	21.12	0.48	0.32	0.3	-	9.46	3.81	0.08	0.42	0.34
Ti6Al4V (% wt.)	-	-	0.04	6.07	Base	3.99	-	-	0.01	-	-

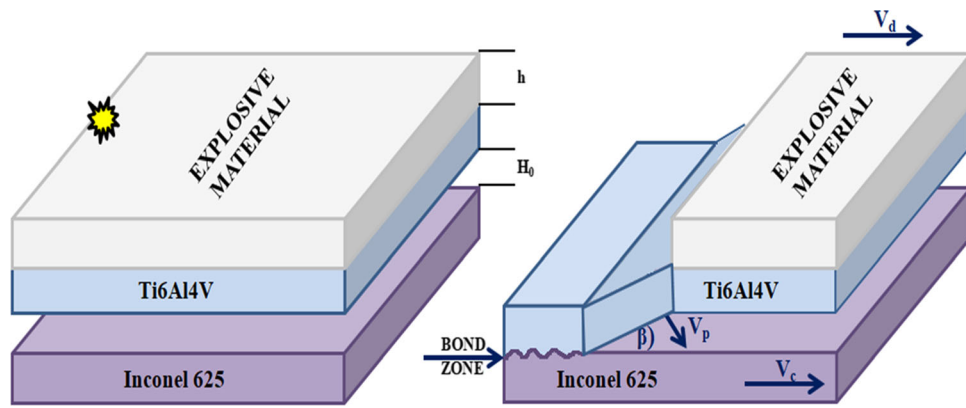


**Fig. 1** Schematic diagram of the explosive welding process of the Ti6Al4V used as the flyer plate, and Inconel 625 as the base plate. The following parameters are used in the process: height of the explosive material ( $h$ ), technological distance between the plates to be joined ( $H_0$ ), angle of deflection of the plate to be joined ( $\beta$ ), velocity of detonation ( $V_d$ ), velocity in the collision area ( $V_c$ ), speed of the plate to be joined ( $V_p$ )

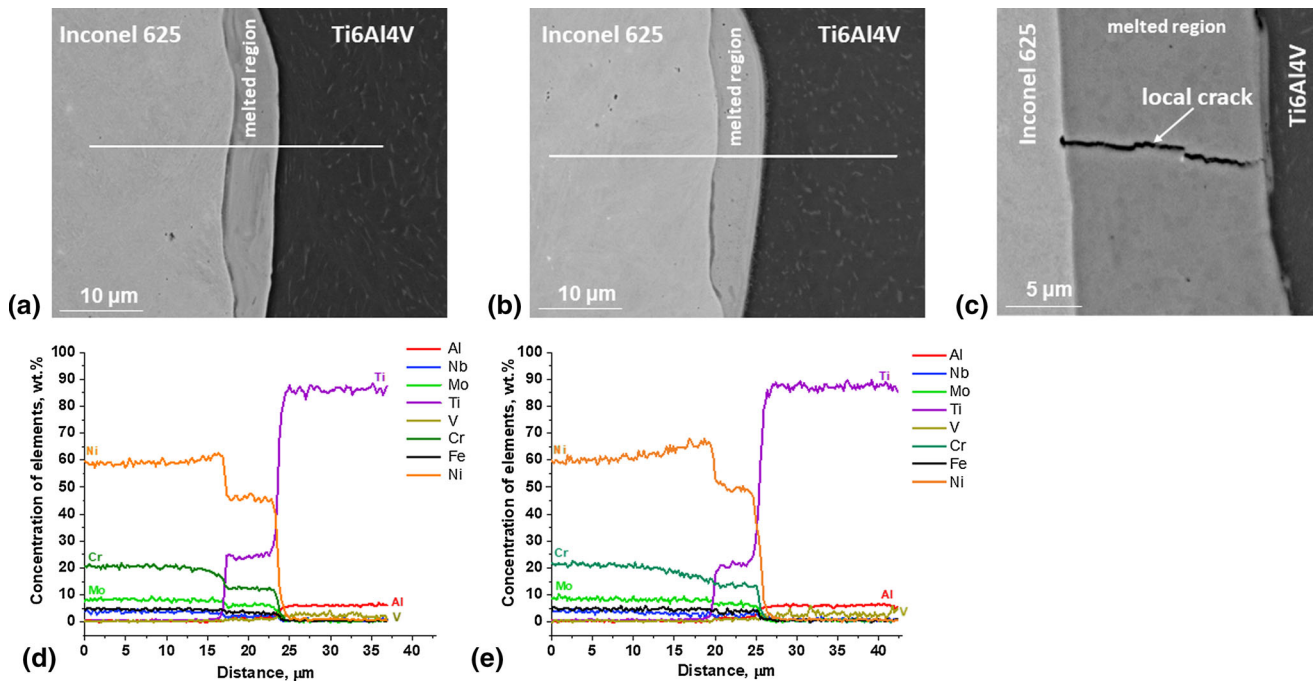


**Fig. 2** SEM-BSE microstructures of the Inconel 625/Ti6Al4V interface after the explosive welding process (a) and after dilatometric measurements (annealing at 873 K for 1 hour) (b) together with the corresponding EDS line-scan located below each image and (c) a local crack visible in the melted region

preserved, locally the large remelted regions taking morphology of the layer appeared. As can be noticed in Fig. 2(c), occasionally the cracks occurred within the remelted regions, but they did not propagate beyond these areas. The line-scan in Fig. 2 manifests the change in the chemical composition across the interface zone. Additionally, the composition of the remelted region, regarding the main elements was:  $43.2 \pm 0.9$  wt.% Ni,  $29.8 \pm 0.6$  wt.% Ti,  $11.4 \pm 0.5$  wt.% Cr ( $38.5 \pm 0.8$  at.% Ni,  $30.9 \pm 0.6$  at.% Ti,  $11.4 \pm 0.5$  at.% Cr), with minor elements: Mo, V, Nb, Al, and Fe. This composition is a mixture of the flyer and base plate materials, with a reduction in nickel and chromium concentration and a substantial increase in titanium (0.4 vs. 29.8 wt.%). Topolski et al. (Ref 6) investigating the same type of weld observed a sharp change in the concentration of the elements across the

Inconel 625 and Ti6Al4V alloys wavy interface, with a large remelting zone formed due to the welding process. It was also interesting to compare the microstructure of the interface zone just after the explosive welding process with the microstructure after dilatometric measurements (see Fig. 2b) to follow possible changes occurring due to the diffusion of elements across the welded zone. However, no significant elemental diffusion was detected by SEM/EDS after dilatometric measurements (annealing at 873 K for 1 hour), as can be compared in Fig. 2(d) and (e).

### 3.2 Corrosion Behavior

In this study, the surface exposed to the corrosion process during the measurements was only Ti6Al4V one. Figure 3 shows the changes in the  $E_{OCP}$  after the immersion of the

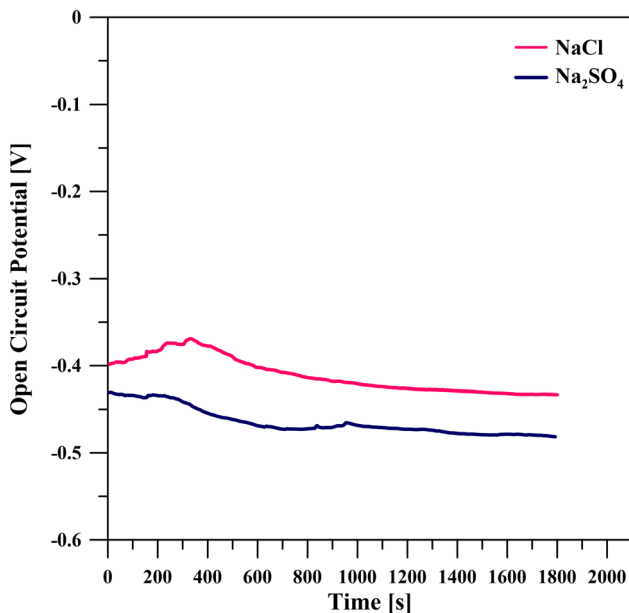


**Fig. 3** Open-circuit potentials ( $E_{OCP}$ ) as a function of time for Ti6Al4V flyer plate determined in 0.5 M Na<sub>2</sub>SO<sub>4</sub> (blue line) solution and 0.5 M NaCl (red line) solution. Measurements were made at 298 K, and the surface of Ti6Al4V was exposed to the corrosion process

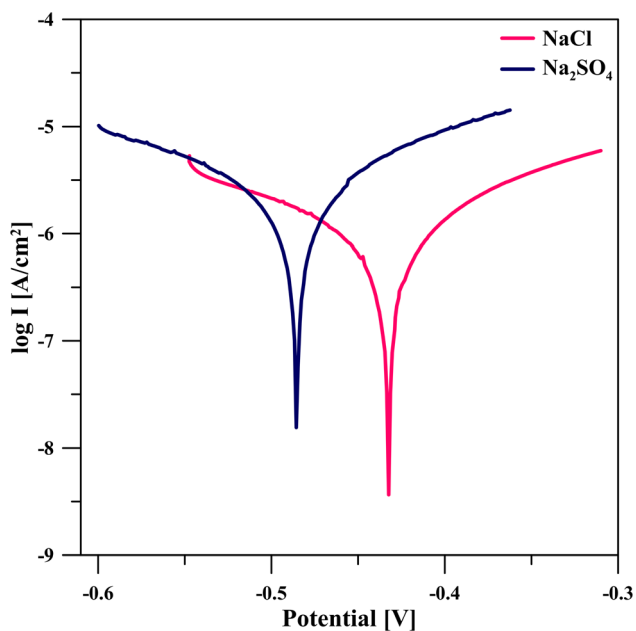


**Fig. 4** Polarization curves in semi-logarithmic coordinates for the Ti6Al4V flyer plate in 0.5 M Na<sub>2</sub>SO<sub>4</sub> (blue line) solution and 0.5 M NaCl (red line). The surface of Ti6Al4V was corroding

sample in the solution for 1800 s. This was the time necessary for the  $E_{OCP}$  value to stabilize. At the beginning, the  $E_{OCP}$  value for both 0.5 M NaCl and 0.5 M Na<sub>2</sub>SO<sub>4</sub> solutions was in the range of 0.40–0.43 V. Based on the collected plot of  $E_{OCP} = f(t)$ , it can be noticed that the potential successively decreased and then reached the equilibrium state. This state stabilized around a potential of  $-0.43$  V for both 0.5 M NaCl (red line) and Na<sub>2</sub>SO<sub>4</sub> (blue line).

The polarization curves (see Fig. 4) show the dependence of the current density on the polarization potential. These curves were used to determine the value of the corrosion current ( $i_{corr}$ ) and the corrosion potential ( $E_{corr}$ ) for the investigated system, by extrapolating the tangents to the anodic and cathodic polarization curves. As can be seen, the red line indicating the 0.5 M NaCl solution is slightly shifted toward the higher potential values. The character of both curves may indicate the behavior typical for the Ti6Al4V alloy at the active–passive transition.

The corrosion parameters obtained from the plotted Tafel diagrams, including corrosion current density ( $j_{corr}$ ), corrosion potential ( $E_{corr}$ ), polarization resistance ( $R_p$ ), and the slope of the anodic ( $b_a$ ) and cathodic ( $b_c$ ) polarization curves are presented in Table 2. The analysis of the presented values shows that the explosively plated Ti6Al4V has very good corrosion resistance, regardless of the used solution. Therefore, it maintained excellent corrosion resistance, as a result of the ease of surface passivation (Ref 12), that is, the formation of a thin layer of Ti oxide on the surface of the material, preventing from direct contact between the metal and the electrolyte, hence the alloy does not undergo rapid corrosion (Ref 13).

The measured corrosion potentials for the NaCl and Na<sub>2</sub>SO<sub>4</sub> solutions were  $-0.433$  V and  $-0.486$  V, respectively. The measurements made with Na<sub>2</sub>SO<sub>4</sub> solution showed a significantly increased corrosion current ( $j_{corr}$ ) of  $10.042 \cdot 10^{-6}$  A/cm<sup>2</sup> compared to  $3.865 \cdot 10^{-6}$  A/cm<sup>2</sup> for the measurements with the use of the NaCl solution. The tested material shows lower corrosion resistance in the environment of Na<sub>2</sub>SO<sub>4</sub> solution. The presence of oxides increases the corrosion resistance. However, the test surfaces were subjected to a grinding process as part of sample preparation before the corrosion tests. Based on data presented in (Ref 12, 14), it can be concluded that the samples prepared in our work for corrosion measurements did not contain an oxide layer. The standard potential of titanium in the voltage series is  $-1.63$  V. This metal can retain its passive properties, not only in solutions containing oxygen but also in solutions containing chloride ions of any concentration.

In order to confirm the experimental results obtained in this study, a model consisting of several elements such as corrosion environment resistance ( $R_s$ ), electrolyte resistance in the deposited layer ( $R_p$ ), layer zone surface capacity ( $C_p$ ), charge transfer resistance at the interface ( $R_{ct}$ ), and electrical double layer capacity ( $CPE_{dl}$ ) was prepared and is presented in Fig. 5.

This model perfectly reproduces the experimental results obtained in the form of fitted electrical circuit elements simulating the electrical and electrochemical properties. The calculated results of electrical parameters of the examined corrosion systems are presented in Table 3, while Fig. 6 shows the Nyquist plots of the collected data. The red line indicates the experimental data, while the blue one the data obtained by the computer simulation.

The calculated data show very good agreement with the experimental data. This proves the correct fitting of the equivalent circuits and their parameters. Particularly noteworthy is the low error value ( $\chi^2$ ), which determines the quality of the measurement and confirms the correctness of the fit of the obtained values. The value of the exponent ( $N$ ) is close to unity typical for capacitors and indicates a very good quality of the passive layer. The capacitor ( $C_p$ ) in the electric circuit model determines the capacitance of the protective layer. This characteristic depends on the thickness of the layer and the electrical permeability of the material.



**Table 2** Corrosion parameters such as  $E_{\text{corr}}$ ,  $j_{\text{corr}}$ , and  $R_p$  were determined for Inconel 625/Ti6Al4V for NaCl and Na<sub>2</sub>SO<sub>4</sub> solutions at room temperature

Solution	$E_{\text{corr}}$ , V	$j_{\text{corr}}$ , A/cm <sup>2</sup>	$b_a$ , V/dec	$b_c$ , V/dec	$R_p$ , Ω·cm <sup>2</sup>
NaCl	− 0.433	3.865·10 <sup>−6</sup>	0.158	0.179	10188
Na <sub>2</sub> SO <sub>4</sub>	− 0.486	10.042·10 <sup>−6</sup>	0.167	0.185	4096

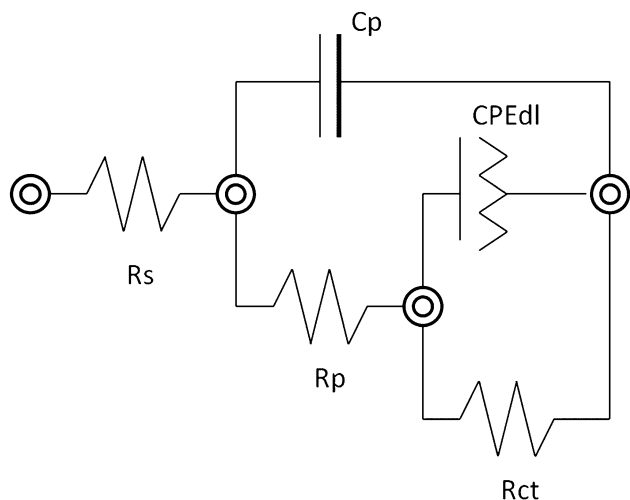


**Fig. 5** Electrical equivalent circuit of a given corrosion system fitted to the data obtained from electrochemical impedance spectroscopy

For a 0.5 M NaCl solution (Fig. 6a), the  $R_s$  is equal to 1.48 Ω·cm<sup>2</sup> and  $R_p$  is equal to 3.73 Ω·cm<sup>2</sup>. During the simulation,  $CPE_{dl}$  was used to better fit the experimental data with the proposed circuit model in both cases. Table 3 contains the equation for calculating the  $CPE_{dl}$  value. In this formula, we use the exponential term  $N$  characterizing the quantity of surface inhomogeneity and the value  $Y_0$  which indicates the value of the admittance of the  $CPE_{dl}$ . The capacity of the surface zone of the layer is 81.48 μF s<sup>N−1</sup> cm<sup>−2</sup>, and the value of  $N$  is equal to 0.705. In the case of the 0.5 M Na<sub>2</sub>SO<sub>4</sub> solution (Fig. 6b), the obtained resistance of the corrosive environment ( $R_s$ ) is 1.01 Ω·cm<sup>2</sup>, while the electrolyte resistance in the Ti6Al4V layer ( $R_p$ ) is equal to 0.96 Ω·cm<sup>2</sup>. The determined capacity of the protective layer is 102.22 μF·s<sup>N−1</sup>·cm<sup>−2</sup>, where  $N= 0.695$ , which may indicate a negligible porosity of the material. The low  $R_s$  value proves the good conductivity of the solutions used. The obtained values of the charge transfer resistance ( $R_{ct}$ ) are consistent with the values of the polarization resistance ( $R_p$ ), resulting from the potentiodynamic measurements, while the value of the  $R_{ct}$  resistance proves an excellent corrosion resistance of the material. Additionally, the semicircle is flattened and its center is below  $Z'$  axis. Depression of the semicircle may result from aspects such as porosity, diffusion phenomena, grain resistance distributions, and local conduction paths. The chi-squared ( $\chi^2$ ) value presented in Table 3 determines the quality of the adjustment of the simulated values to the obtained experimental data. Low  $\chi^2$  values confirm the very good agreement between the simulated values and the obtained experimental data, which proves a correct fit of the equivalent systems and their parameters.

A significant flattening of the semicircles, for both solutions, may indicate that surface area after the impact underwent strong plastic deformation, therefore, grain boundaries may play role in the formation of such semicircles shape. In the case of the presented semicircles, shown in the form of Nyquist plots (Fig. 6), it is noted that the one obtained for the Na<sub>2</sub>SO<sub>4</sub> solution has the smallest diameter. This proves the highest corrosion resistance of Ti6Al4V in the studied environment and confirms the results obtained potentiodynamically.

### 3.3 Dilatometric Results

For comparison, samples for dilatometric studies of thermal expansion and linear coefficient of thermal expansion ( $\alpha$ ) were cut perpendicular and parallel to the direction of propagation of the detonation wave. Additionally, the measurements were also performed for two reference samples: Inconel 625 and Ti6Al4V (each layer of weld separately) in the same temperature range and heating rate as the tested platers' samples. Each specimen was measured three times on both the Ti6Al4V and the Inconel 625 layer sides. Figure 7 presents the obtained results, and Table 4 summarizes the average values of the  $\alpha$  in the studied temperature ranges.

Generally, the linear coefficient of thermal expansion of a material increases with the increasing temperature of the process because the potential energy characterizing interatomic interactions increases with increasing distance between atoms (Ref 15). When a phase, allotropic, or polymorphic transition occurs in a material, the values of the  $\alpha$  and thermal expansion change rapidly (a sharp increase or decrease of their values), caused by a change in the packing of the crystallographic lattice of the material after and before the transition (Ref 15–17). In the case of the investigated platers, the obtained results present only a linear relation of the thermal expansion coefficient with temperature, which suggests the lack of phase transitions in the sample in the whole investigated temperature range.

The values of thermal expansion and  $\alpha$  of measured samples, shown in Fig. 7, obtained by cutting parallel or perpendicular to the direction of the explosion are similar, which indicates that the direction of their cut does not matter. This observation is not surprising since, in most of the polycrystalline materials, the thermal expansion is an isotropic property, i.e., it does not depend on which direction it is measured.

The performed dilatometric measurements show that the studied layered samples have the values of thermal expansion between those of the reference materials (Inconel 625 and Ti6Al4V). The value of thermal expansion of pure Inconel 625 is, according to the available literature, more than 40% higher than that for pure Ti6Al4V alloy in the temperature range up to 373 K (Ref 18, 19); with the higher temperature range, this difference increases. It should be also noted that samples measured from the Inconel 625 layer side of the plater obtain a thermal expansion value slightly lower than that for pure

**Table 3** The obtained parameter values for the models of optimal equivalent circuits in two different solutions

Solution	$R_s, \Omega\cdot\text{cm}^2$	$R_p, \Omega\cdot\text{cm}^2$	$R_{ct}, \Omega\cdot\text{cm}^2$	$C_p, \text{nF}/\text{cm}^2$	$CPE_{dl}$		$\chi^2$
					$Y, \mu\text{F s}^{N-1}/\text{cm}^2$	$N$	
NaCl	1.48	3.72	6237	18333	81.48	0.705	0.0211
Na <sub>2</sub> SO <sub>4</sub>	1.01	0.96	2636	7222	102.22	0.695	0.0045

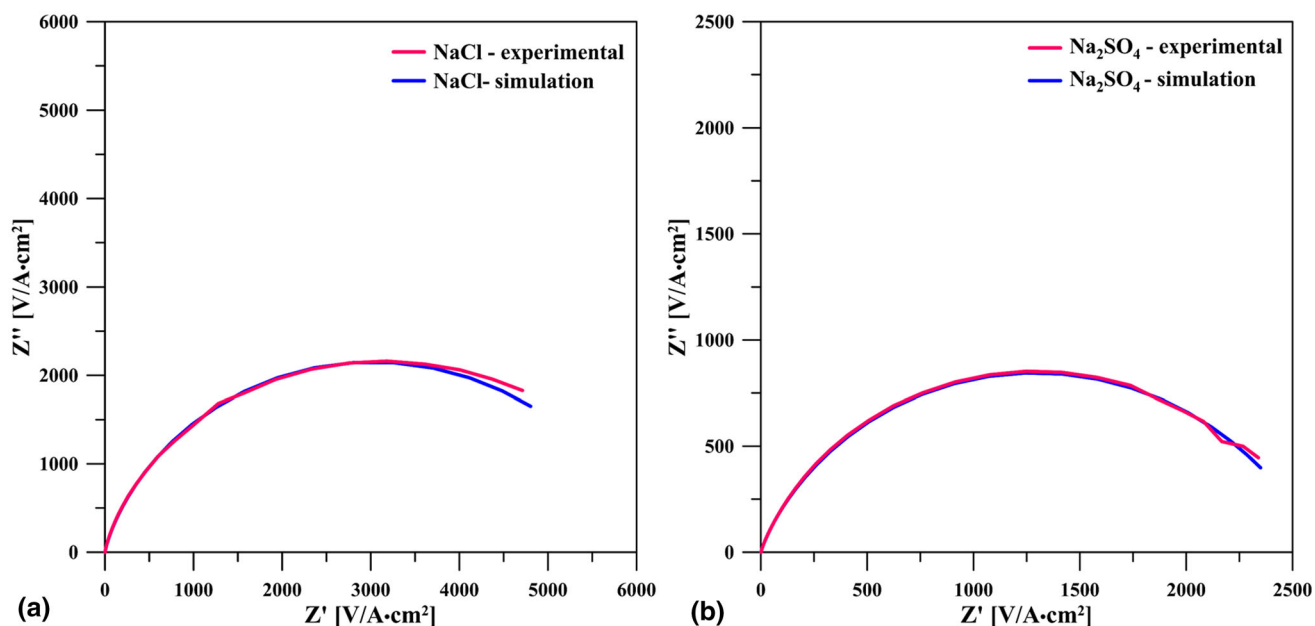


**Fig. 6** Comparison of experimental impedance data for the Ti6Al4V flyer plate presented in the Nyquist plot with computer simulations. Data for (a) NaCl and (b) Na<sub>2</sub>SO<sub>4</sub> solution

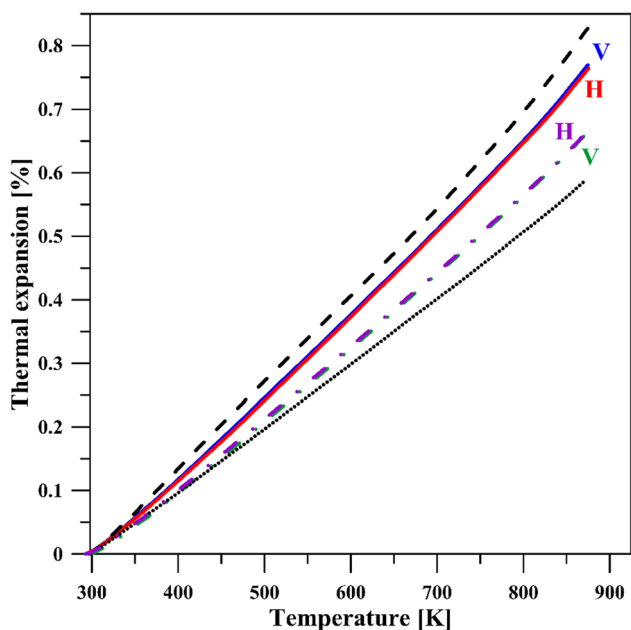


**Fig. 7** Thermal expansion of the test plater specimen as a function of temperature; solid lines (blue and red) represent samples measured from the Inconel 625 layer side; the dashed-dotted lines represent the results of samples from the Ti6Al4V layer side; V and H represent samples cut parallel and perpendicular to the direction of the explosion, respectively; The dashed and dotted lines are the thermal expansion values of the reference samples, Inconel 625 and Ti6Al4V, respectively

Inconel 625, and samples measured from the Ti6Al4V layer side receive higher values compared to those for the Ti6Al4V pure layer. This observation may suggest that the remelted zone occurring between the Inconel 625 and Ti6Al4V plates has a small effect on the expansion of the material. Most probably, these remelted zones formed as a result of explosive welding block the free expansion of the material with increasing temperature, and thus the whole material has a different thermal expansion than pure unbonded materials.

#### 4. Conclusions

By using the explosive welding method, Inconel 625 was successfully clad with Ti6Al4V flyer plate. A continuous interface was formed along the entire bonding zone with local melted regions with the composition of  $43.2 \pm 0.9$  wt.% Ni,  $29.8 \pm 0.6$  wt.% Ti,  $11.4 \pm 0.5$  wt.% Cr with minor elements: Mo, V, Nb, Al, and Fe. This composition stayed almost unchanged after annealing of the weld at 600 °C for 1 h (dilatometric experiment).

The corrosion tests of the Inconel 625/Ti6Al4V weld carried out for the Ti6Al4V flyer plate surface showed that the potentiodynamic measurements and the analysis using electrochemical impedance spectroscopy were consistent and showed the same trend in corrosion properties. Furthermore, the selected electrical equivalent circuit generated impedance spectra convergent with the frequency characteristics of

**Table 4** Average the thermal expansion coefficient of investigated platers

Temperature range, K	The average thermal expansion coefficient $\alpha \cdot 10^{-6}, \text{K}^{-1}$		The standard deviation for thermal expansion coefficient $u(\alpha) \cdot 10^{-6}, \text{K}^{-1}$	
	V*	H**	V*	H**
<i>The results for samples measured from the side of the Inconel 625 layer</i>				
298-373	10.63	10.70	0.20	0.16
298-473	11.76	11.75	0.24	0.15
298-573	12.33	12.23	0.39	0.06
298-673	12.52	12.51	0.26	0.05
298-773	12.76	12.78	0.24	0.06
298-873	13.15	13.20	0.20	0.08
<i>The results for samples measured from the side of the Ti6Al4V layer</i>				
298-373	9.31	9.11	0.25	0.13
298-473	10.32	10.10	0.21	0.16
298-573	10.69	10.54	0.24	0.13
298-673	10.92	10.82	0.24	0.12
298-773	11.15	11.07	0.20	0.10
298-873	11.49	11.46	0.20	0.05

\*The values of the samples cut parallel to the direction of the explosion  
\*\*The values of the samples cut perpendicular to the direction of the explosion

corrosion systems determined experimentally for the entirely studied frequency range. Significantly higher corrosion resistance of the Ti6Al4V material was found for the NaCl solution ( $4096 \Omega \cdot \text{cm}^2$ ) in comparison to  $\text{Na}_2\text{SO}_4$  solution ( $10188 \Omega \cdot \text{cm}^2$ ) used as the corrosive environment. The corrosion potential of the Ti6Al4V surface tested in sodium chloride solution ( $j_{\text{corr}} = 3.865 \cdot 10^{-6} \text{ A/cm}^2$ ) was slightly higher compared to the value obtained for the sodium sulfate solution ( $j_{\text{corr}} = 10.042 \cdot 10^{-6} \text{ A/cm}^2$ )

Thermal expansion measurements of the investigated Inconel 625/Ti6Al4V weld, made with an optical and horizontal dilatometer, in the temperature range from 298 to 873 K, showed similar values of linear thermal expansion coefficient of samples cut parallel or perpendicular to the direction of the explosion. Tested layered samples have  $\alpha$  values between those of initial alloy materials (Inconel 625 and Ti6Al4). Moreover, the obtained results of thermal expansion with temperature show linear character in the whole applied temperature range, implying the absence of phase transitions of the weld in the used temperature range. This stays in agreement with SEM/EDS observations of the interfaces of the tested samples.

### Acknowledgments

This research was financially supported by the Institute of Metallurgy and Materials Science of the Polish Academy of Sciences (IMIM PAS) within the statutory work “The interface zone of Inconel 625/Ti6Al4V obtained with the use of explosion energy” Z-5/2020. The purchase of the optical dilatometer Misura® 3 FLEX-ODLT, which was used in the investigations, was financed by the European Regional Development Fund within the frames of Project POIG. 02.01.00-12-175/09. SEM/EDS and dilatometric studies were performed in the Accredited Testing Laboratories at the Institute of Metallurgy and Materials Science of the Polish Academy of Sciences.

### References

1. C. Leyens and M. Peters, *Titanium and titanium alloys: fundamentals and applications*, Wiley VCH Verlag GmbH & Co, 2003. <https://doi.org/10.1002/3527602119>
2. C. Kuphasuk, Y. Oshida, C.J. Andres, S.T. Hovijitra, M.T. Barco and D.T. Brown, Electrochemical Corrosion of Titanium and Titanium-Based Alloys, *J. Prosthet. Dent.*, 2001, **85**(2), p 195–202. <https://doi.org/10.1067/mp.2001.113029>
3. R.W. Schutz, C.F. Baxter, P.L. Boster and F.H. Fores, Applying Titanium Alloys in Drilling and Offshore Production Systems, *JOM*, 2001, **53**, p 33–35. <https://doi.org/10.1007/s11837-001-0145-1>
4. P. Corigliano and V. Crupi, Fatigue Analysis of Ti6AL4V/INCONEL 625 Dissimilar Welded Joints, *Ocean Eng.*, 2021, **221**, 108582. <http://doi.org/10.1016/j.oceaneng.2021.108582>
5. A.K. Rai, A. Kumar, V. Shankar, T. Jayakumar, K. Bhanu Sankara Rao and B. Raj, Characterization of Microstructures in Inconel 625 Using x-ray Diffraction Peak Broadening and Lattice Parameter Measurements, *Scr. Mater.*, 2004, **51**, p 59–63. <https://doi.org/10.1016/j.scripta.mat.2004.03.017>
6. K. Topolski, Z. Szulc and H. Garbacz, Microstructure and Properties of the Ti6Al4V/Inconel 625 Bimetal Obtained by Explosive Joining, *J. Mater. Eng. Perform.*, 2016, **25**, p 3231–3237. <https://doi.org/10.1007/s11665-016-2080-x>
7. Z. Sun, X. Ji, W. Zhang, L. Chang, G. Xie, H. Chang and L. Zhou, Microstructure Evolution and High Temperature Resistance of Ti6Al4V/Inconel625 Gradient Coating Fabricated by Laser Melting Deposition, *Mater. Des.*, 2020. <https://doi.org/10.1016/j.matdes.2020.108644>
8. B.B. Sherpa, D.K.B. Pal and U. Batra, Study of the explosive welding process and applications, In: *Advances in applied physical and chemical sciences-a sustainable approach Chapter: 5* Publisher: Excel-ent Publishing House, New Delhi (2014)
9. T.Z. Blazynski, *Explosive welding, forming and compaction*, Springer, London and New York, 1983
10. S. Terlicka, A. Dębski, A. Budziak, M. Zabrocki and W. Gąsior, Structural and Physical Studies of the Ag-Rich Alloys from Ag-Li System, *Thermochim. Acta.*, 2019, **673**, p 185–191. <https://doi.org/10.1016/j.tca.2019.01.016>
11. S. Terlicka, A. Dębski, W. Gierlotka, A. Wierzbička-Miernik, A. Budziak, A. Sypien, M. Zabrocki and W. Gąsior, Structural and Physical Studies of the Ag-Rich Alloys from Ag-Li System, *Calphad*, 2020, **68**, 101739. <https://doi.org/10.1016/j.calphad.2020.101739>

12. D. Prando, A. Brenna, M.V. Diamanti, S. Beretta, F. Bolzonii, M. Ormellese and M.P. Pedefferri, Corrosion of Titanium: Part 1: Aggressive Environments and Main Forms of Degradation, *J. Appl. Biomater. Funct. Mater.*, 2017, **15**, p 291–302. <https://doi.org/10.5301/jabfm.5000387>
13. S. Barril, S. Mischler and D. Landolt, Electrochemical Effects on the Fretting Corrosion Behaviour of Ti6Al4V in 0.9% Sodium Chloride Solution, *Wear*, 2005, **259**, p 282–291. <https://doi.org/10.1016/j.wear.2004.12.012>
14. A. Leon, G.K. Levy, T. Ra, A. Shirizly and E. Aghion, The Effect of Strain Rate on Stress Corrosion Performance of Ti6Al4V Alloy Produced by Additive Manufacturing Process, *J. Mater. Res. Technol.*, 2002, **9**, p 4097–4105. <https://doi.org/10.1016/j.jmrt.2020.02.035>
15. Y.S. Touloukian, R.K. Kirby, R.E. Taylor and P.D. Desai, Thermal expansion: metallic elements and alloys, *Thermophysical Properties of Matter*, Vol 12, Y.S. Touloukian, C.Y. Ho Ed., New York, Plenum, 1977
16. M.D. Mathews, A.K. Tyagi and P.N. Moorthy, Study of Phase Transition in REOF System by Dilatometry (RE = La, Nd, Sm, Gd, Eu and Y), *Thermochim. Acta.*, 1997, **298**, p 165–167. [https://doi.org/10.1016/S0040-6031\(97\)00200-1](https://doi.org/10.1016/S0040-6031(97)00200-1)
17. B.N. Wani, M.D. Mathews and U.R.K. Rao, Polymorphism in Tripotassium Lanthanate Hexafluorides (Ln = Sm, Eu, Gd, Tb and Er), *Thermochim. Acta.*, 1995, **265**, p 141–149. [https://doi.org/10.1016/0040-6031\(95\)02409-U](https://doi.org/10.1016/0040-6031(95)02409-U)
18. Special Metals Corporation Products. INCONEL® alloy 625; <https://www.specialmetals.com/assets/smc/documents/alloys/inconel/inconel-alloy-625.pdf>; Accessed April 2021
19. R. Boyer, G. Welsch and E.W. Collings, *Materials Properties Handbook: Titanium Alloys*, 1st ed. ASM International, Materials Park OH, 1994

**Publisher's Note** Springer Nature remains neutral with regard to jurisdictional claims in published maps and institutional affiliations.